



The *lhfp15* Ohnologs *lhfp15a* and *lhfp15b* Are Required for Mechanotransduction in Distinct Populations of Sensory Hair Cells in Zebrafish

Timothy Erickson^{1,2*}, Itallia V. Pacentine², Alexandra Venuto¹, Rachel Clemens² and Teresa Nicolson^{2†}

¹ Department of Biology, East Carolina University, Greenville, NC, United States, ² Oregon Hearing Research Center and Vollum Institute, Oregon Health and Science University, Portland, OR, United States

OPEN ACCESS

Edited by:

Isabel Varela-Nieto,
Spanish National Research Council
(CSIC), Spain

Reviewed by:

Hiroshi Hibino,
Niigata University, Japan
Sangyong Jung,
Singapore Bioimaging Consortium
(A*STAR), Singapore
Gwenaëlle Geleoc,
Harvard Medical School,
United States

*Correspondence:

Timothy Erickson
ericksonti17@ecu.edu

† Present address:

Teresa Nicolson,
Otolaryngology-Head and Neck
Surgery, Stanford School of Medicine,
Stanford, CA, United States

Received: 11 September 2019

Accepted: 16 December 2019

Published: 15 January 2020

Citation:

Erickson T, Pacentine IV,
Venuto A, Clemens R and Nicolson T
(2020) The *lhfp15* Ohnologs *lhfp15a*
and *lhfp15b* Are Required
for Mechanotransduction in Distinct
Populations of Sensory Hair Cells
in Zebrafish.
Front. Mol. Neurosci. 12:320.
doi: 10.3389/fnmol.2019.00320

Hair cells sense and transmit auditory, vestibular, and hydrodynamic information by converting mechanical stimuli into electrical signals. This process of mechano-electrical transduction (MET) requires a mechanically gated channel localized in the apical stereocilia of hair cells. In mice, lipoma HMGIC fusion partner-like 5 (LHFPL5) acts as an auxiliary subunit of the MET channel whose primary role is to correctly localize PCDH15 and TMC1 to the mechanotransduction complex. Zebrafish have two *lhfp15* genes (*lhfp15a* and *lhfp15b*), but their individual contributions to MET channel assembly and function have not been analyzed. Here we show that the zebrafish *lhfp15* genes are expressed in discrete populations of hair cells: *lhfp15a* expression is restricted to auditory and vestibular hair cells in the inner ear, while *lhfp15b* expression is specific to hair cells of the lateral line organ. Consequently, *lhfp15a* mutants exhibit defects in auditory and vestibular function, while disruption of *lhfp15b* affects hair cells only in the lateral line neuromasts. In contrast to previous reports in mice, localization of Tmc1 does not depend upon Lhfp15 function in either the inner ear or lateral line organ. In both *lhfp15a* and *lhfp15b* mutants, GFP-tagged Tmc1 and Tmc2b proteins still localize to the stereocilia of hair cells. Using a stably integrated GFP-Lhfp15a transgene, we show that the tip link cadherins Pcdh15a and Cdh23, along with the Myo7aa motor protein, are required for correct Lhfp15a localization at the tips of stereocilia. Our work corroborates the evolutionarily conserved co-dependence between Lhfp15 and Pcdh15, but also reveals novel requirements for Cdh23 and Myo7aa to correctly localize Lhfp15a. In addition, our data suggest that targeting of Tmc1 and Tmc2b proteins to stereocilia in zebrafish hair cells occurs independently of Lhfp15 proteins.

Keywords: hair cell, mechanotransduction, deafness, lateral line, zebrafish, LHFPL5, TMC1, PCDH15

INTRODUCTION

The mechano-electrical transduction (MET) complex of sensory hair cells is an assembly of proteins and lipids that facilitate the conversion of auditory, vestibular and hydrodynamic stimuli into electrical signals. Our current understanding is that the proteins of the MET complex consist of the tip link proteins cadherin 23 (CDH23) and protocadherin 15 (PCDH15) at the upper

and lower ends of the tip link respectively (Kazmierczak et al., 2007), the pore-forming subunits transmembrane channel-like proteins TMC1 and TMC2 (Kawashima et al., 2011; Pan et al., 2013, 2018), and the accessory subunits transmembrane inner ear (TMIE) and lipoma HMGIC fusion partner-like 5 (LHFPL5) (Xiong et al., 2012; Zhao et al., 2014; Cunningham and Müller, 2019). How these proteins are correctly localized to the sensory hair bundle and assemble into a functional complex is a fundamental question for understanding the molecular basis of how mechanotransduction occurs.

Recent studies have revealed extensive biochemical interactions between the MET complex proteins that are required for the function and/or stable integration of each component in the complex. In particular, LHFPL5 is a central player in MET complex formation, stability, and function. LHFPL5 (a.k.a. tetraspan membrane protein of the hair cell stereocilia/TMHS) is a four transmembrane domain protein from the superfamily of tetraspan junctional complex proteins. This superfamily includes junctional proteins like claudins and connexins, as well as ion channel auxiliary subunits such as transmembrane α -amino-3-hydroxy-5-methyl-4-isoxazole propionic acid receptor (AMPA) regulatory proteins (TARPs) and the gamma subunits of voltage gated calcium channels. Pathogenic mutations in LHFPL5 are a cause of non-syndromic sensorineural hearing loss in humans (DFNB67), mice and zebrafish (Nicolson et al., 1998; Longo-Guess et al., 2005; Shabbir et al., 2006; Obholzer et al., 2012). LHFPL5 localizes to the tips of stereocilia (Xiong et al., 2012; Mahendrasingam et al., 2017; Li et al., 2019) where it directly interacts with other MET complex components. Co-immunoprecipitation experiments in heterologous cells suggests that LHFPL5 can directly interact with PCDH15 and TMIE (Xiong et al., 2012; Zhao et al., 2014). A structure of the PCDH15 – LHFPL5 complex has also been reported (Ge et al., 2018).

A precise role for LHFPL5 has yet to be defined. One current hypothesis is that LHFPL5 acts as an auxiliary subunit of the MET channel to stabilize the complex, similar to TARPs and the gamma subunits of voltage-gated calcium channels. In mouse cochlear hair cells, PCDH15 and LHFPL5 require each other for stable localization at the tips of stereocilia (Xiong et al., 2012; Mahendrasingam et al., 2017), consistent with their well-defined biochemical interaction. The partial loss of PCDH15 from the stereocilia explains the observed reduction in the number of tip links and the dysmorphic hair bundles in *Lhfp15*^{-/-} hair cells. Interestingly, although experiments have failed to demonstrate a biochemical interaction between LHFPL5 and the TMCs, LHFPL5 is required for the localization of TMC1, but not TMC2, in the hair bundle of mouse cochlear hair cells (Beurg et al., 2015). Consistent with this finding, the researchers identified a residual TMC2-dependent MET current in *Lhfp15* mutant mice. The basis for the selective loss of TMC1 is not known.

In zebrafish, *Lhfp15a* plays a similar role in mechanotransduction as its mammalian counterparts. A mutation in zebrafish *lhfp15a* was reported in a forward genetic screen for genes required for hearing and balance (Nicolson et al., 1998; Obholzer et al., 2012). The loss of *Lhfp15a* disrupts the targeting of *Pcdh15a* to stereocilia and results in

splayed hair bundles (Maeda et al., 2017). However, *Lhfp15a* is not required to correctly localize Tmc1 and vice versa (Pacentine and Nicolson, 2019), in spite of their biochemical interaction in cultured cells (Xiong et al., 2012). *Lhfp15* still localizes to the tips of stereocilia in *Tmc1/Tmc2* double mutants (Beurg et al., 2015), as well as *transmembrane O-methyltransferase (tomt)* mouse and zebrafish mutants, which fail to traffic TMCs to the hair bundle (Cunningham et al., 2017; Erickson et al., 2017). This phenotype suggests that *Lhfp15* localization does not require the TMCs. However, a number of questions regarding the functions of *Lhfp15* remain unanswered: (1) In zebrafish, what are the molecular requirements for targeting *Lhfp15a* to the hair bundle? (2) Is the *Lhfp15*-dependent targeting of Tmc1 to the hair bundle an evolutionarily conserved aspect of their interaction? (3) *lhfp15a* mutants have defects in auditory and vestibular behaviors, yet sensory hair cells of the lateral line are unaffected (Nicolson et al., 1998). What is the genetic basis for the persistence of lateral line function in *lhfp15a* mutants?

In this work, we report that teleost fish have two *lhfp15* genes, *lhfp15a* and *lhfp15b*. The zebrafish *lhfp15* ohnologs are expressed in distinct populations of larval sensory hair cells: *lhfp15a* in the auditory and vestibular system; *lhfp15b* in the hair cells of the lateral line organ. Their divergent expression patterns explain why lateral line hair cells are still mechanically sensitive in *lhfp15a* mutants. CRISPR-Cas 9 knockout of *lhfp15b* alone silences the lateral line organ but has no effect on otic hair cell function. We also show that neither *Lhfp15a* nor *Lhfp15b* are required for Tmc localization in stereocilia. Additionally, we use a GFP-tagged *Lhfp15a* to demonstrate that *Myo7aa* and the tip link proteins *Cdh23* and *Pcdh15a* are required for proper *Lhfp15a* localization in otic hair cell bundles. This study reveals the subfunctionalization of the zebrafish *lhfp15* ohnologs through the divergence in their expression patterns. Furthermore, our work complements previous results from murine cochlear hair cells by highlighting a conserved association between *Lhfp15* and *Pcdh15*, but also demonstrating novel requirements for *Cdh23* and *Myo7aa* in localizing *Lhfp15a*. Lastly, our work indicates that *Lhfp15*-dependent localization of Tmc1 is not a universal feature of sensory hair cells and that *Lhfp15* proteins are required for mechanotransduction independently of a role in localizing the Tmc channel subunits to stereocilia.

MATERIALS AND METHODS

Ethics Statement

Animal research complied with guidelines stipulated by the Institutional Animal Care and Use Committees at Oregon Health and Science University (Portland, OR, United States) and East Carolina University (Greenville, NC, United States). Zebrafish (*Danio rerio*) were maintained and bred using standard procedures (Westerfield, 2000).

Mutant and Transgenic Fish Lines

The following zebrafish mutant alleles were used for this study: *cdh23*ⁿ¹⁹, *cdh23*^{tj264}, *lhfp15a*^{tm290d}, *lhfp15b*^{vo35}, *myo7aa*^{ty220},

pcdh15a^{psi7}, *pcdh15a^{th263b}* (Nicolson et al., 1998; Ernest et al., 2000; Obholzer et al., 2012; Erickson et al., 2017; Maeda et al., 2017). The transgenic lines used in this study were *Tg(-6myo6b:eGFP-lhfp15a)vo23Tg*, *Tg(-6myo6b:tmc1-emGFP)vo27Tg*, *Tg(-6myo6b:tmc2b-emGFP)vo28Tg* (Erickson et al., 2017), and *Tg(-6myo6b:eGFP-pA)vo68Tg*. All experiments used larvae at 1–7 dpf, which are of indeterminate sex at this stage.

Genotyping

Standard genomic PCR followed by Sanger sequencing was used to identify *cdh23^{tj264}*, *cdh23^{nl9}*, *lhfp15a^{tm290d}*, *pcdh15a^{psi7}*, and *pcdh15a^{th263b}* alleles. The *lhfp15b^{vo35}* mutation disrupts a MluCI restriction site (AATT) and we are able to identify *lhfp15b^{vo35}* hetero- and homozygotes based on the different sizes of MluCI-digested PCR products resolved on a 1.5% agarose gel. The following primers were used for genotyping:

cdh23^{nl9}: Fwd – CCACAGGAATTCTGGTGTCC, Rvs – GAAAGTGGGCGTCTCATCAT;
cdh23^{tj264}: Fwd – GGACGTCAGTGTTTCATGGTG, Rvs – TTTTCTGACCGTGGCATTAAAC;
lhfp15a^{tm290d}: Fwd – GGACCATCATCTCCAGCAAAC, Rvs – CACGAAACATATTTTCATCACCAG;
lhfp15b^{vo35}: Fwd – GCGTCATGTGGGCAGTTTTC, Rvs – TAGACACTAGCGGCGTTGC;
myo7a^{ty220}: Fwd – TAGGTCCTCTTTAATGCATA, Rvs – GTCTGTCTGTCTGTCTATCTGTCTCGCT;
pcdh15a^{psi7}: Fwd – TTGGCACCCTATCTTTACCG, Rvs – ACAGAAGGCACCTGGAAAAC;
pcdh15a^{th263b}: Fwd – AGGGACTAAGCCGAAGGAAG, Rvs – CACTCATCTTCACAGCCATACAG.

Phylogeny

Lhfp15 protein sequences retrieved from either NCBI or Ensembl (**Supplementary Table 1**). Phylogenetic analysis was done on www.phylogeny.fr using T-Coffee (multiple sequence alignment), GBLOCKS (alignment curation), PhyML (maximum likelihood tree construction with 100 replicates to estimate bootstrap values), and TreeDyn (visualization) (Dereeper et al., 2008).

mRNA *in situ* Hybridization

lhfp15a and *lhfp15b* probe templates were amplified from total RNA using the following primers: *lhfp15a* Fwd: AATATTGGTGCATAGACTCAAGGAGG; Rvs: GACTCCAA AATGACCTTTTAACAAACGC. *lhfp15b* Fwd: TGAAGAT CAGCTACGATATAACCGG; Rvs: ACTGTGATTGGTGTA TTTCCAGC. The inserts were cloned into the pCR4 vector for use in probe synthesis. mRNA *in situ* probe synthesis and hybridization was performed essentially as previously described (Thisse and Thisse, 2008; Erickson et al., 2010). Stained specimens were mounted on a depression slide in 1.2% low-melting point agarose and imaged on a Leica DMLB microscope fitted with a Zeiss AxioCam MRc 5 camera using Zeiss AxioVision acquisition software (Version 4.5).

Immunofluorescent Staining, FM Dye Labeling, and Fluorescence Microscopy

Anti-Pcdh15a immunostaining and FM dye labeling of inner ear and lateral line hair cells were performed as previously described (Erickson et al., 2017). All fluorescent imaging was done on Zeiss LSM 700 or LSM 800 laser scanning confocal microscopes. Z-stacks were analyzed using ImageJ (Schneider et al., 2012). All related control and experimental images were adjusted equally for brightness and contrast in Adobe Photoshop CC.

CRISPR-Cas9 Knockout of *lhfp15b*

An sgRNA targeting the *lhfp15b* sequence 5'-CAACCCAATCACCTCGGAAT-3' was synthesized essentially as described (Gagnon et al., 2014). For microinjection, 1 µg of sgRNA was mixed with 1 µg of Cas9 protein and warmed to 37°C for 5 min to promote the formation of the Cas9-sgRNA complex. Approximately 2 nl of this solution was injected into wild type embryos at the single-cell stage. Efficacy of cutting was determined in two ways: (1) Single larvae genotyping - Amplification of the target genomic region by PCR and running the products on 2.5% agarose gels to assay for disruption of a homogenous amplicon. (2) Assaying for disruption of the mechanotransduction channel in lateral line hair cells by FM 1-43 dye uptake. Larvae displaying a non-wild type pattern of FM 1-43 dye uptake were raised to adulthood. Progeny from in-crosses of F0 adults were exposed to FM 1-43 dye to identify founders. By outcrossing founder adults, we established a line of fish carrying a 5 base pair deletion in the *lhfp15b* coding region that causes a S77FfsX48 mutation (*lhfp15b^{vo35}*). This mutation disrupts the protein in the first extracellular loop and deletes the final three of four transmembrane helices in Lhfp15b.

Acoustic Startle Response

Quantification of the larval acoustic startle response was performed using the Zebrabox monitoring system (ViewPoint Life Sciences, Montreal, Canada) as previously described (Maeda et al., 2017) with the following modifications. Each trial included six larvae which were subjected to two or three trials of 6 acoustic stimuli. For each individual larva, the trial with best AEBR performance was used for quantification. Positive responses where spontaneous movement occurred in the second prior to the stimulus were excluded from analysis. Trials where spontaneous movement occurred for more than 6 of the 12 stimuli were also excluded from analysis.

Microphonics

We performed the microphonic measurements as previously described (Pacentine and Nicolson, 2019). In brief, we anesthetized 3 dpf larvae in extracellular solution [140 mM NaCl, 2 mM KCl, 2 mM CaCl₂, 1 mM MgCl₂, and 10 mM 4-(2-hydroxyethyl)-1-piperazineethanesulfonic acid (HEPES); pH 7.4] containing 0.02% 3-amino benzoic acid ethylester (MESAB; Western Chemical). We pinned the larvae with two glass fibers straddling the yolk and a third perpendicular fiber to prevent sliding. For pipettes, we used borosilicate glass with filament,

O.D.: 1.5 mm, O.D.: 0.86 mm, 10 cm length (Sutter, item # BF150-86-10, fire polished). Using a Sutter Puller (model P-97), we created recording pipettes with a long shank with a resistance of 10–20 M Ω , after which we beveled the edges to a resistance of 4–5 M Ω using a Sutter Beveler with impedance meter (model BV-10C). For the glass probe delivering the piezo stimulus, we pulled a long shank pipette and fire polished to a closed bulb. We shielded the apparatus with tin foil to completely ground the piezo actuator. To maintain consistent delivery of stimulus, we always pressed the probe to the front of the head behind the lower eye, level with the otoliths in the ear of interest. We also maintained a consistent entry point dorsal to the anterior crista and lateral to the posterior crista. During delivery of stimulus, the piezo probe made light contact with the head. We drove the piezo with a High Power Amplifier (piezosystem jena, System ENT/ENV, serial # E18605), and recorded responses in current clamp mode with a patch-clamp amplifier (HEKA, EPC 10 usb double, serial # 550089). Voltage responses were amplified 1000x and filtered between 0.1 – 3000 Hz by the Brownlee Precision Instrumentation Amplifier (Model 440). We used a 200 Hz sine wave stimulus at 10 V and recorded at 20 kHz, collecting 200 traces per experiment. Each stimulus was of 40 ms duration, with 20 ms pre- and post-stimulus periods. The piezo signal was low-pass filtered at 500 Hz using the Low-Pass Bessel Filter 8 Pole (Warner Instruments). In Igor Pro, we averaged each set of 200 traces to generate one wave response per larva. To quantify hair cell activity, we calculated the amplitude from base-to-peak of the first peak. Larvae were genotyped as described above.

Hair Cell Counts

lhfp15b^{vo35/+} fish were crossed with *Tg(myo6b:eGFP-pA)vo68Tg; lhfp15b*^{vo35/+} fish to produce wild type and *lhfp15b*^{vo35} siblings expressing green fluorescent protein in hair cells. Wild type and *lhfp15b* mutant larvae were sorted by FM 4-64 labeling ($n = 11$ each). In experiment 1, larvae ($n = 5$ each genotype) were fixed in 4% paraformaldehyde at 5 dpf. In experiment 2, larvae ($n = 6$ each genotype) were imaged immediately. *lhfp15a*^{tm290d/+} fish were in-crossed to produce wild type and *lhfp15a*^{tm290d} siblings. Larvae were sorted based on the auditory and vestibular defects associated with the *lhfp15a*^{tm290d} homozygous mutants. Larvae were labeled with FM 1-43 ($n = 6$ each). For all experiments, specimens were mounted in low melting point agarose and the L1, M1, and O2 neuromasts were imaged on a Zeiss LSM 800 confocal. Cell counts were performed using the Z-stack data.

Statistics

Statistical analyses were done using the R stats package in RStudio (RStudio Team, 2018; R Core Team, 2019). P -values of less than 0.05 were considered to be statistically significant. Plots were made with ggplot2 (Wickham, 2016).

Data Availability

The raw data supporting the conclusions of this article will be made available by the corresponding author, without undue reservation, to any qualified researcher.

RESULTS

Teleost Fish Have Ohnologous *lhfp15* Genes

Genes that have been duplicated as a result of a whole genome duplication (WGD) event are known as *ohnologs* (Ohno, 1970; Wolfe, 2000). Due to the teleost-specific WGD, it is not uncommon to find ohnologous genes in teleost fish where other vertebrate classes possess a single gene. The *Danio rerio* (zebrafish) genome contains two *lhfp15* genes: *lhfp15a* (ENSDARG00000045023) and *lhfp15b* (ENSDARG00000056458). To determine if *lhfp15* duplication is general to the teleost lineage, we queried either GenBank or Ensembl databases to collect Lhfp15 protein sequences for humans, mice, chick, frogs, and representative sequences from 14 phylogenetic orders of ray-finned fish (Actinopterygii), including 13 orders from the Teleostei infraclass and one from the Holostei infraclass (Supplementary Table 1). The latter (Spotted gar, *Lepisosteus oculatus*) is commonly used to infer the consequences of the teleost WGD, since the Holostei and Teleostei infraclasses diverged before the teleost WGD (Braasch et al., 2016). Phylogenetic analysis of the Lhfp15 protein sequences supports the idea that duplicate *lhfp15* genes originated from the teleost WGD event (Figure 1A). In all 13 teleost orders surveyed, there are two *lhfp15* genes whose protein products cluster with either the *lhfp15a* or *lhfp15b* ohnolog groups. Based on available genomic data, there is no evidence that spotted gar fish have duplicated *lhfp15* genes. Nor is there evidence that the Salmonid-specific WGD (Allendorf and Thorgaard, 1984) lead to further expansion of the *lhfp15* family. These analyses suggest that the ancestral *lhfp15* gene was duplicated in the teleost WGD and that the *lhfp15* ohnologs were retained in all teleost species examined here.

Alignment of the zebrafish Lhfp15a and Lhfp15b proteins with those from human, mouse and chicken reveals that both zebrafish ohnologs retain the same protein structure (Figure 1B). Zebrafish Lhfp15a and Lhfp15b are 76% identical and 86% similar to one another (Needleman-Wunsch alignment). Compared to human LHFPL5, Lhfp15a and Lhfp15b are 70/65% identical and 86/81% similar respectively. The ENU-generated mutation in *lhfp15a* (*tm290d*) (Obholzer et al., 2012) is indicated by the red triangle (K80X). To investigate the function of *lhfp15b*, we generated a Cas9-induced lesion in the *lhfp15b* gene in a similar location as the *tm290d* mutation. We recovered a line with a 5 base pair deletion leading to a frameshift mutation (*lhfp15b*^{vo35}, red square; S77FfsX48).

lhfp15a and *lhfp15b* Are Expressed in Distinct Populations of Sensory Hair Cells

To characterize the spatial and temporal patterns of *lhfp15a/b* gene expression, we performed whole mount mRNA *in situ* hybridization on zebrafish larvae at 1, 2, and 5-days post-fertilization (dpf) (Figure 2). After 1 day of development, there are nascent hair cells of the presumptive anterior and posterior maculae in the developing ear, but no lateral line hair cells at this stage. We detect *lhfp15a* expression in the presumptive anterior

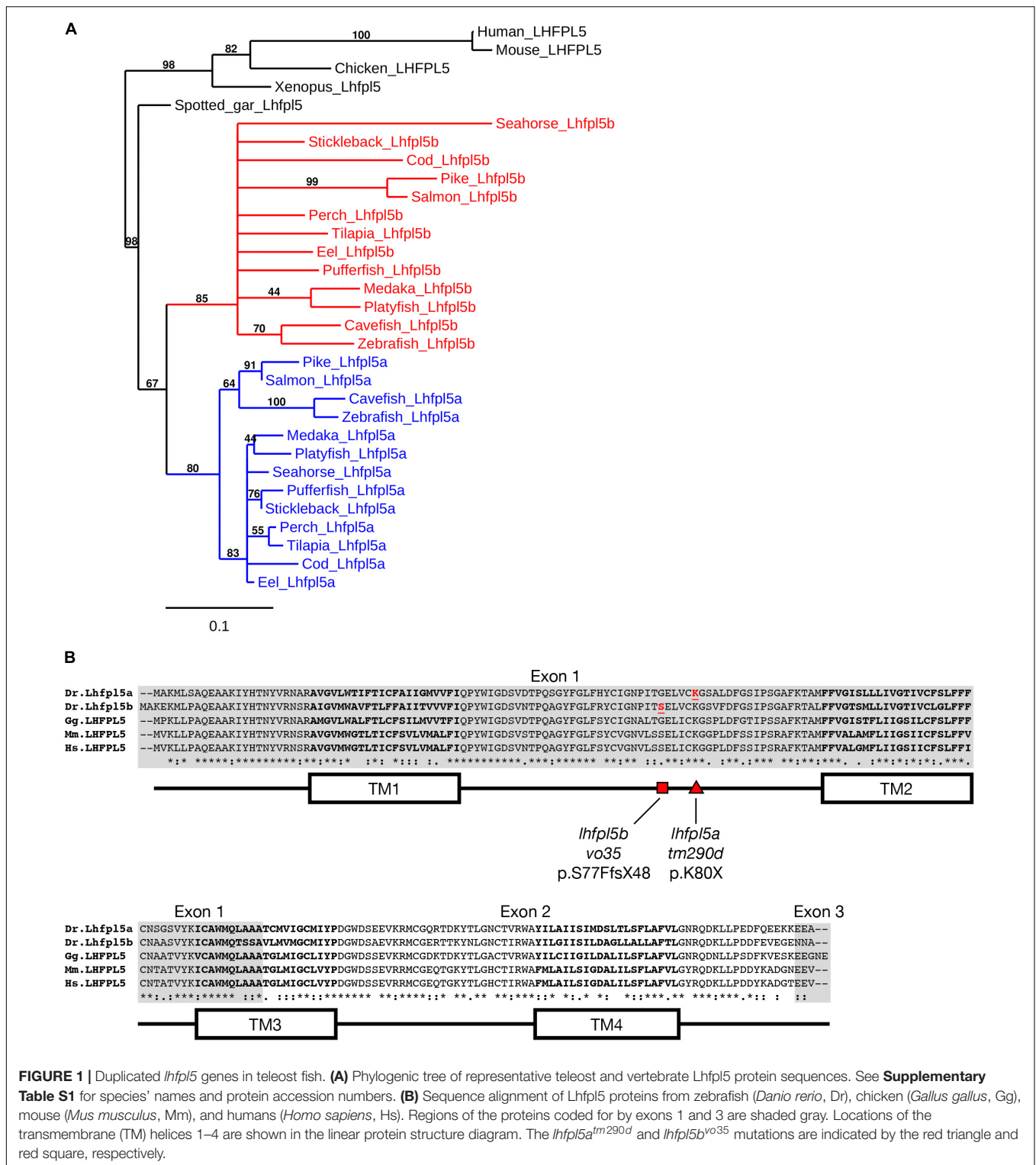
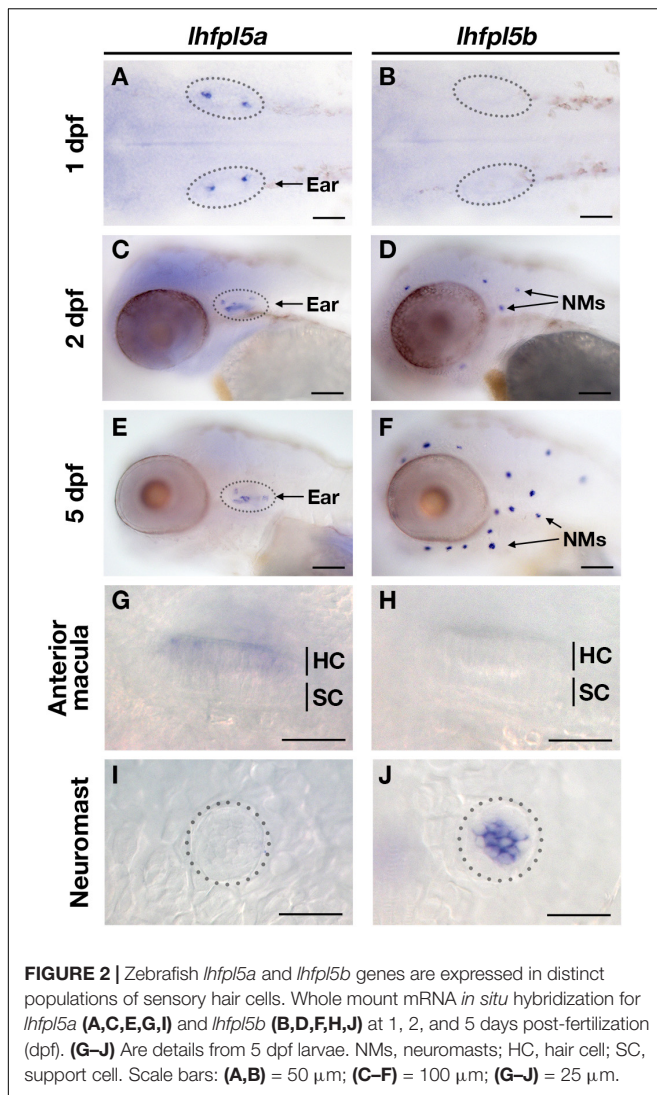


FIGURE 1 | Duplicated *lhfp15* genes in teleost fish. **(A)** Phylogenetic tree of representative teleost and vertebrate Lhfp15 protein sequences. See **Supplementary Table S1** for species' names and protein accession numbers. **(B)** Sequence alignment of Lhfp15 proteins from zebrafish (*Danio rerio*, Dr), chicken (*Gallus gallus*, Gg), mouse (*Mus musculus*, Mm), and humans (*Homo sapiens*, Hs). Regions of the proteins coded for by exons 1 and 3 are shaded gray. Locations of the transmembrane (TM) helices 1–4 are shown in the linear protein structure diagram. The *lhfp15a*^{tm290d} and *lhfp15b*^{vo35} mutations are indicated by the red triangle and red square, respectively.

and posterior maculae at 1 dpf (**Figure 2A**). No signal for *lhfp15b* was observed at this time point (**Figure 2B**). At 2 dpf, we observe a clear distinction in the expression patterns of the *lhfp15a* and *lhfp15b* genes (**Figures 2C,D**). *lhfp15a* continues to be expressed in the ear, but expression is not observed in the newly deposited

neuromasts. Conversely, we detect *lhfp15b* expression exclusively in neuromasts at this stage, both on the head (**Figure 2D**) and trunk (data not shown). This divergence in *lhfp15* ohnolog expression continues at 5 dpf, with *lhfp15a* found exclusively in the sensory patches of the ear and *lhfp15b* restricted to lateral line



hair cells (Figures 2E–J). Taken together, our results suggest that both *lhfp15a* and *lhfp15b* have been retained since the teleost WGD because of their non-overlapping mRNA expression patterns.

lhfp15a Mediates Mechanosensitivity of Otic Hair Cells

lhfp15a^{tm290d} (*astronaut/asn*) mutants were initially characterized by balance defects, an absence of the acoustic startle reflex, and a lack of brainstem Ca²⁺ signals after acoustic startle. However, neuromast microphonic potentials were normal (Nicolson et al., 1998). In light of our *in situ* hybridization data (Figure 2), these results suggest that *lhfp15a* is required for auditory and vestibular hair cell function only. To test this possibility, we performed several functional assays measuring the activity of hair cells in the otic capsule. First, we tested macular hair cell activity (Lu and DeSmidt, 2013; Yao et al., 2016) by recording extracellular microphonic potentials from the inner ears of *lhfp15a*^{tm290d} mutants, along with wild type and *lhfp15b*^{vo35} larvae at 3 dpf. We then measured baseline-to-peak amplitude of the

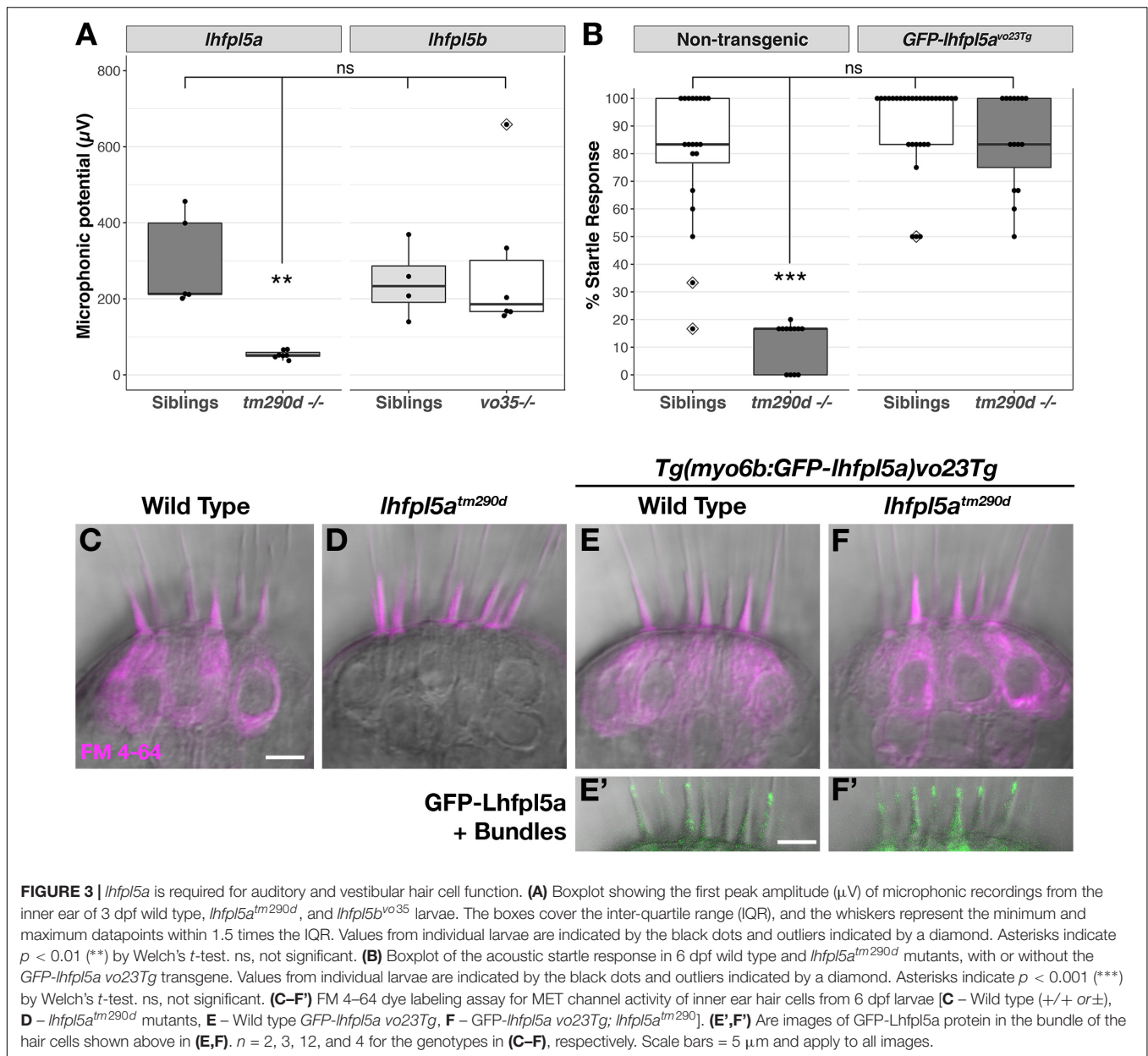
first peak to quantify activity (Supplementary Figures 1A–D). Consistent with the initial characterization of the behavioral defects in *lhfp15a*^{tm290d} mutants, we did not detect robust microphonic potentials from the inner ear of *lhfp15a*^{tm290d} mutants (Figure 3A). We measured an average first peak microphonic of 53.1 μ V from *lhfp15a*^{tm290d} mutants ($n = 7$), which was significantly less than the 296.2 μ V average value of their WT siblings ($n = 5$; $p = 0.01$, Welch's *t*-test). We believe that at least some of the signal detected in *lhfp15a*^{tm290d} mutants may be a stimulus artifact due the unusual rise time and similar observations we have made in other known transduction-null mutants.

For the *lhfp15b*^{vo35} mutants ($n = 6$), we measured an average first peak microphonic potential of 280.9 μ V. These values were not significantly different from their WT siblings ($n = 4$, average 243.8 μ V; $p = 0.7$) but were significantly greater than the *lhfp15a*^{tm290d} mutants ($p = 0.036$). Thus, *lhfp15a*^{tm290d} mutants exhibit defects in inner ear function, while the *lhfp15b*^{vo35} mutation has no effect on these hair cells. To further confirm the lack of inner ear function in *lhfp15a*^{tm290d} mutants, we performed an acoustic startle test on larvae at 6 dpf (Figure 3B). Results confirm that *lhfp15a*^{tm290d} mutants are profoundly deaf, displaying little to no response to acoustic stimuli ($p < 0.001$ compared to all other genotypes). Finally, we examined the basal MET channel activity of hair cells of the inner ear by injecting FM 4–64 into the otic capsule and imaging the lateral cristae sensory patch. WT hair cells readily labeled with FM 4–64 whereas *lhfp15a*^{tm290d} mutant cells showed no sign of dye internalization (Figures 3C,D). These three tests confirmed that all sensory patches in the otic capsule are inactive in *lhfp15a*^{tm290d} mutants.

A GFP-*lhfp15a* transgenic line of zebrafish – *Tg(myo6b:eGFP-lhfp15a)vo23Tg* – has been reported previously (Erickson et al., 2017). GFP-Lhfp15a is present at the tips of stereocilia, similar to the localization observed for mouse LHFPL5 (Xiong et al., 2012; Mahendrasingam et al., 2017). To demonstrate that the GFP-Lhfp15a protein is functional, we assayed for rescue of the acoustic startle reflex and MET channel activity in homozygous *lhfp15a*^{tm290d} mutants expressing the transgene. The startle reflex of *lhfp15a*^{tm290d} mutants expressing GFP-Lhfp15a were statistically indistinguishable from non-transgenic and transgenic WT siblings ($p = 0.48$ and 0.26 respectively; Figure 3B). Likewise, FM 4–64 dye-labeling in the inner ear was restored to *lhfp15a*^{tm290d} mutants expressing GFP-Lhfp15a (Figures 3E–F'). From these results we conclude that the hair bundle-localized GFP-Lhfp15a protein is functional and can rescue the behavioral and MET channel defects in *lhfp15a*^{tm290d} mutants.

lhfp15b Mediates Mechanosensitivity of Lateral Line Hair Cells

The divergent expression patterns of the *lhfp15* ohnologs suggests that *lhfp15b* alone may be mediating mechanosensitivity of lateral line hair cells. To test this, we compared basal MET channel activity in neuromast hair cells of WT, *lhfp15a*^{tm290d} and *lhfp15b*^{vo35} larvae using an FM 1–43 dye uptake assay (Figures 4A–C). Strikingly, lateral line hair cells in *lhfp15b*^{vo35}



mutants do not label with FM 1–43 while there is no difference in the intensity of FM 1–43 labeling of hair cells between WT and *lhfp15a*^{tm290d} mutants (Figures 4A–C and Supplementary Figures 2A–C). We quantified this loss of lateral line function in *lhfp15b* mutants by measuring the average FM 1–43 fluorescence intensity per hair cell in each imaged neuromast of *lhfp15b*^{vo35} mutants and wild type siblings at 2 dpf (Figures 4D,E,H) and 5 dpf (Figures 4F–H). *lhfp15b*^{vo35} mutants exhibit a statistically significant decrease in FM 1–43 uptake at both 2 and 5 dpf (Welch's *t*-test, $p < 0.001$ both time points). While there is negligible FM dye labeling in the vast majority of *lhfp15b*^{vo35} mutant neuromasts, we occasionally observe labeling in some hair cells, most reproducibly in the SO3 neuromast. Occasional labeling persists in *lhfp15a*/*lhfp15b* double mutants, indicating

that *lhfp15a* is not partially compensating for the loss of *lhfp15b* (Supplementary Figures 3A–D). The loss of MET channel activity in *lhfp15b*^{vo35} neuromasts is rescued by expression of the *GFP-lhfp15a vo23Tg* transgene (Figures 4I,J; $n = 7/7$ mutant individuals). This result indicates that Lhfp15a and Lhfp15b are functionally interchangeable in this context.

We have previously reported a reduced number of neuromast hair cells in other transduction mutants such as *myo7aa* (*mariner*), *pcdh15a* (*orbiter*), and *tomt* (*mercury*) (Seiler et al., 2005; Erickson et al., 2017). The ultimate cause for this reduction in hair cell number is not known. If *lhfp15b*^{vo35} mutants are defective in mechanotransduction, we would expect a similar decrease in the number of neuromast hair cells. To test this idea, we compared hair cell counts between wild type, *lhfp15a*^{tm290d},

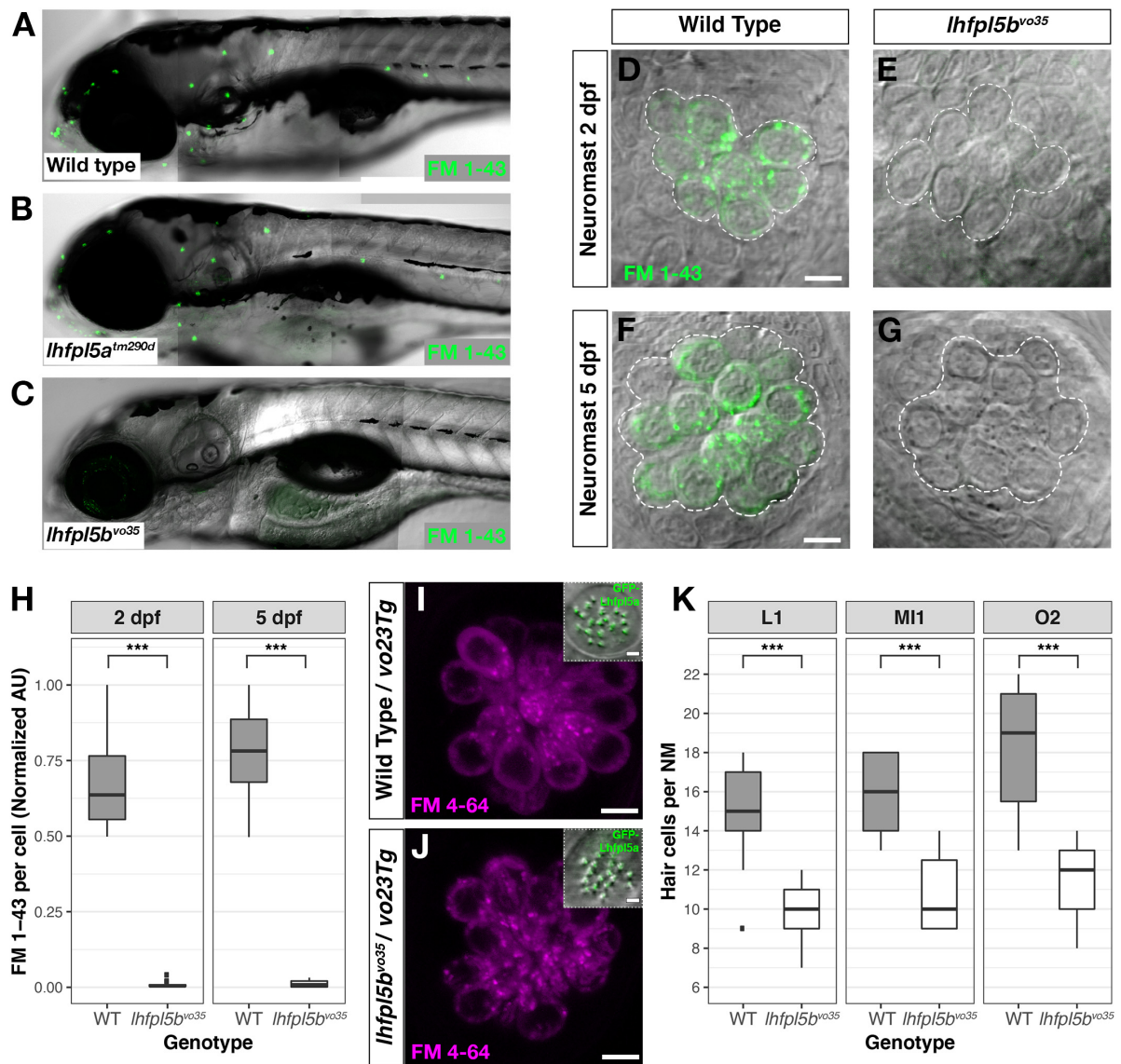


FIGURE 4 | *lhfp15b* is required for lateral line hair cell function. (A–C) Representative images of 5 dpf zebrafish larvae (A – Wild type; B – *lhfp15a^{tm290d}*; C – *lhfp15b^{vo35}*) labeled with the MET channel-permeant dye FM 1–43. (D–G) Representative images of individual neuromasts from 2 and 5 dpf wild type and *lhfp15b^{vo35}* larvae labeled with FM 1–43. Dashed lines outline the cluster of hair cells in each neuromast. (H) Quantification of normalized FM 1–43 fluorescence intensity per hair cell of 2 and 5 dpf neuromasts ($n = 10$ WT, 14 *lhfp15b^{vo35}* NMs at 2 dpf; $n = 6$ WT, 13 *lhfp15b^{vo35}* NMs each genotype at 5 dpf). The box plots cover the inter-quartile range (IQR), and the whiskers represent the minimum and maximum datapoints within 1.5 times the IQR. Asterisks indicate $p < 0.001$ (***) by Welch's t -test. (I, J) Rescue of FM dye labeling in *lhfp15b^{vo35}* mutants ($n = 7$) by the GFP-*Lhfp15a* (*vo23Tg*) transgene. The GFP-*Lhfp15a* bundle and FM 4–64 images are from the same NM for each genotype. (K) Quantification of hair cell number in L1, MI1, and O2 neuromasts from 5 dpf *lhfp15b^{vo35}* mutants ($n = 11$) and wild-type siblings ($n = 11$). The box plots are the same as in (H). Asterisks indicate $p < 0.001$ (***) by Welch's t -test. Scale bars = 5 μ m, applies to (D–G, I, J); 2 μ m in (I, J) insets.

and *lhfp15b^{vo35}* larvae at 5 dpf. As expected, wild type and *lhfp15a^{tm290d}* mutants have statistically equivalent numbers of hair cells in the neuromasts surveyed (Supplementary Figure 2D, $p = 0.58$). In *lhfp15b^{vo35}* mutant neuromasts, we observe a statistically significant decrease in the number of hair cells (Figure 4K, $n = 11$ individuals per genotype, 3 NM each, $p < 0.001$ each NM type by Welch's t -test; representative neuromasts are shown in Supplementary Figure 4). This decrease in the number of neuromast hair cells is consistent

with *lhfp15b* mutants being deficient in mechanotransduction in this cell type.

Lhfp15 Is Not Required for Tmc Localization to the Hair Bundle in Zebrafish Hair Cells

Previous studies have demonstrated that loss of LHFPL5 leads to a $\sim 90\%$ reduction in the peak amplitude of the transduction

current in mouse cochlear outer hair cells (Xiong et al., 2012). Single channel recordings from *Lhfp15* mutants revealed that the remaining transduction current in *Lhfp15* mutants was mediated by TMC2 (Beurg et al., 2015). Using antibodies to detect endogenous protein, TMC1 was found to be absent from the bundle of *Lhfp15* mouse mutants. However, injectoprotected Myc-TMC2 was still able to localize to the hair bundle, supporting the idea that LHFPL5 is required for the targeting of TMC1, but not TMC2. The localization of exogenously expressed TMC1 in *Lhfp15* mutants was not reported.

To determine if the Tmcs require *Lhfp15a* for localization to the hair bundle of zebrafish hair cells, we bred stable transgenic lines expressing GFP-tagged versions of Tmc1 (*vo27Tg*) and Tmc2b (*vo28Tg*) (Erickson et al., 2017) into the *lhfp15a^{tm290d}* mutant background and imaged Tmc localization in the lateral cristae of the ear. In contrast to what was observed in mouse cochlear hair cells, both Tmc1-GFP and Tmc2b-GFP are still targeted to the hair bundle in *lhfp15a^{tm290d}* mutants ($n = 11/11$ and $9/9$ individuals respectively; **Figures 5A–D'**). We also observe Tmc2b-GFP localization in the neuromast hair bundles of *lhfp15b^{vo35}* mutants ($n = 7/7$ individuals; **Figures 5E–F'**). Additionally, we do not observe any rescue of hair cell function in *lhfp15b* mutants expressing the Tmc2b-GFP protein (**Supplementary Figures 5A–C**). As such, these results suggest that GFP-tagged Tmc1 and Tmc2b do not require *Lhfp15* for hair bundle localization in zebrafish hair cells.

GFP-*Lhfp15a* Localization in Stereocilia Requires *Pcdh15a*, *Cdh23*, and *Myo7aa*

Previous work has shown that PCDH15 and LHFPL5 are mutually dependent on one another to correctly localize to the site of mechanotransduction in mouse cochlear hair cells (Xiong et al., 2012; Mahendrasingam et al., 2017). Likewise in zebrafish, *Lhfp15a* is required for proper *Pcdh15a* localization in the hair bundle, as determined *Pcdh15a* immunostaining and the expression of a *Pcdh15a*-GFP transgene in *lhfp15a^{tm290d}* mutants (Maeda et al., 2017). Using the previously characterized antibody against *Pcdh15a*, we observe the highest level of *Pcdh15a* staining at the apical part of the hair bundle, with less intense punctate staining throughout the stereocilia in 3 dpf wild type larvae (**Figure 6A**). *lhfp15a^{tm290d}* mutants exhibit splayed hair bundles, with low levels of *Pcdh15a* staining restricted to the tip of each stereocilium ($n = 5/5$ individuals; **Figure 6B**), confirming our previous report.

To determine if *Lhfp15a* also depends on *Pcdh15a* for its localization, we imaged GFP-*Lhfp15a* in the lateral cristae of *pcdh15a^{psi7}* homozygous mutants. In wild type larvae, GFP-*Lhfp15a* is distributed throughout the hair bundle at the tips of stereocilia (yellow arrow heads), with a higher intensity of GFP evident in the tallest rows, possibly at the sites of kinociliary links (**Figures 6C,C'**, arrow). In *pcdh15a^{psi7}* mutants, GFP-*Lhfp15a* is absent from the hair bundle except for the tallest rows of stereocilia adjacent to the kinocilium ($n = 4$ individuals; **Figures 6D,D'**, arrow). We observed similar results using the *pcdh15a^{th263b}* allele ($n = 6/6$ individuals; **Supplementary Figures 6A,B'**). Consistent with our earlier

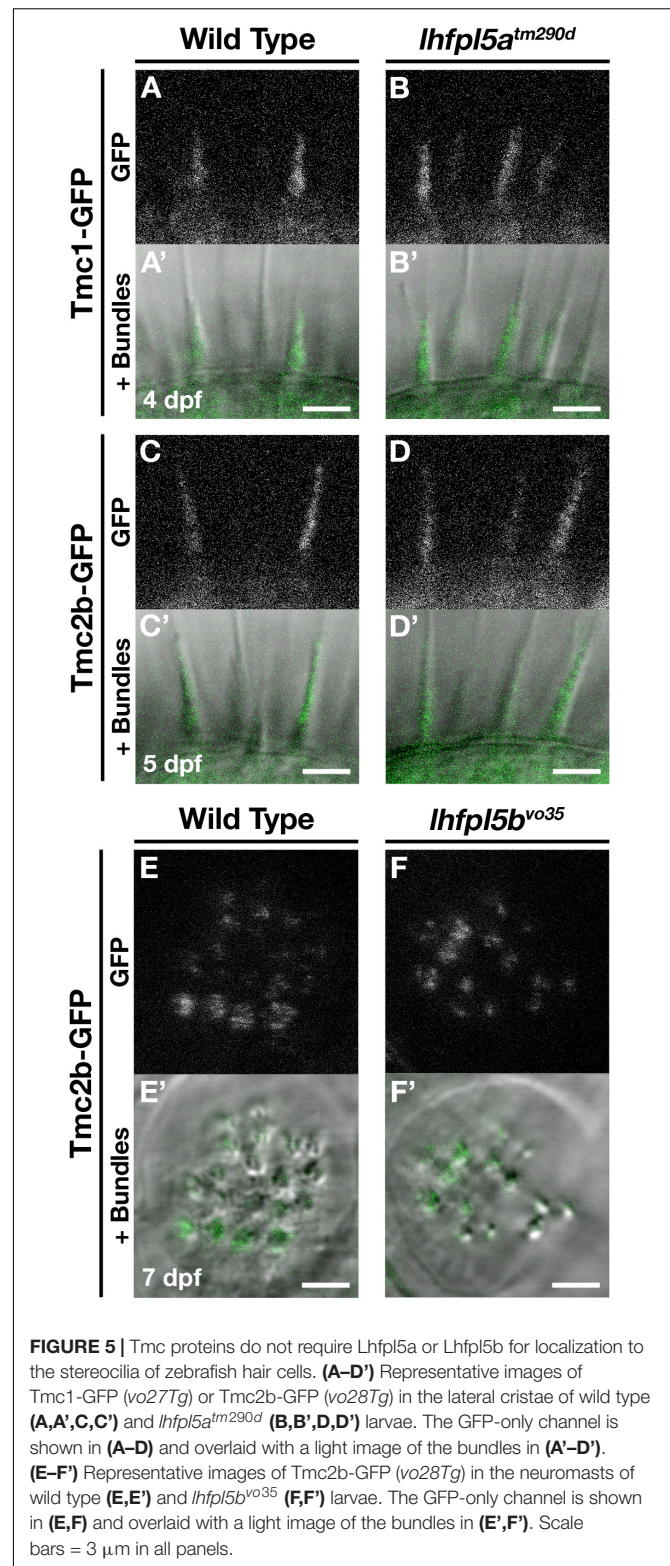


FIGURE 5 | Tmc proteins do not require *Lhfp15a* or *Lhfp15b* for localization to the stereocilia of zebrafish hair cells. **(A–D')** Representative images of Tmc1-GFP (*vo27Tg*) or Tmc2b-GFP (*vo28Tg*) in the lateral cristae of wild type **(A,A',C,C')** and *lhfp15a^{tm290d}* **(B,B',D,D')** larvae. The GFP-only channel is shown in **(A–D)** and overlaid with a light image of the bundles in **(A'–D')**. **(E–F')** Representative images of Tmc2b-GFP (*vo28Tg*) in the neuromasts of wild type **(E,E')** and *lhfp15b^{vo35}* **(F,F')** larvae. The GFP-only channel is shown in **(E,F)** and overlaid with a light image of the bundles in **(E',F')**. Scale bars = 3 μ m in all panels.

studies (Seiler et al., 2005; Maeda et al., 2017), we observe splayed hair bundles in both *pcdh15a* alleles suggesting a loss of connections and tip links between the stereocilia. These results

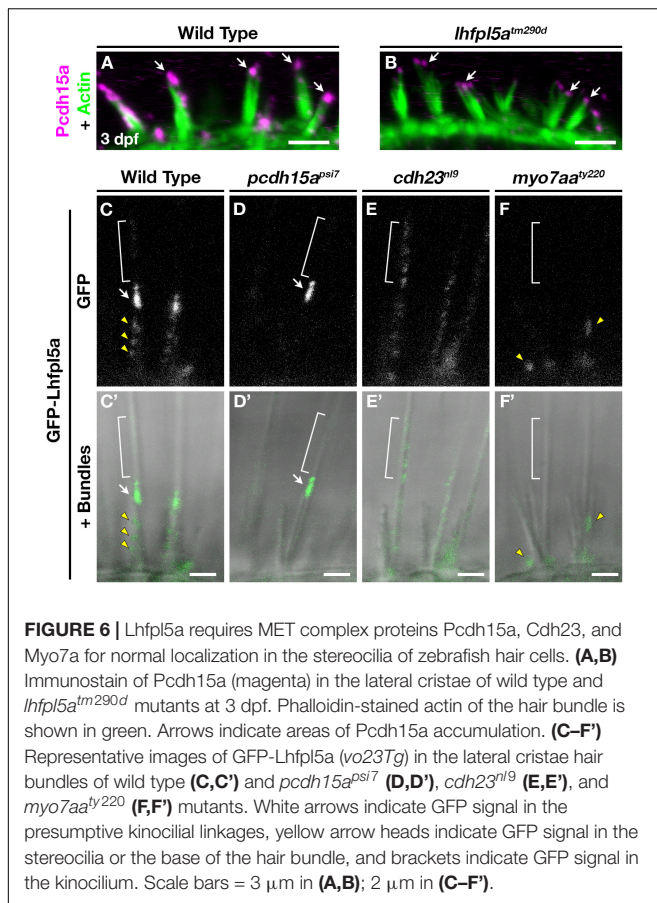


FIGURE 6 | Lhfp15a requires MET complex proteins Pcdh15a, Cdh23, and Myo7a for normal localization in the stereocilia of zebrafish hair cells. **(A,B)** Immunostain of Pcdh15a (magenta) in the lateral cristae of wild type and *lhfp15a^{tm290d}* mutants at 3 dpf. Phalloidin-stained actin of the hair bundle is shown in green. Arrows indicate areas of Pcdh15a accumulation. **(C-F')** Representative images of GFP-Lhfp15a (*vo23Tg*) in the lateral cristae hair bundles of wild type **(C,C')** and *pcdh15a^{psi7}* **(D,D')**, *cdh23ⁿ¹⁹* **(E,E')**, and *myo7aa^{ty220}* **(F,F')** mutants. White arrows indicate GFP signal in the presumptive kinociliary linkages, yellow arrowheads indicate GFP signal in the stereocilia or the base of the hair bundle, and brackets indicate GFP signal in the kinocilium. Scale bars = 3 μm in **(A,B)**; 2 μm in **(C-F')**.

indicate that GFP-Lhfp15a requires Pcdh15a for stable targeting to the shorter stereocilia, but Pcdh15a is not required for retaining GFP-Lhfp15a in the tallest rows of stereocilia adjacent to the kinocilium.

The observation that some GFP-Lhfp15a signal remains in the tallest stereocilia of *pcdh15a* mutants suggests that additional proteins are involved in targeting Lhfp15a to these sites in zebrafish vestibular hair cells. Previous research has shown that mouse CDH23 still localizes to tips of stereocilia in PCDH15-deficient mice (Boëda et al., 2002; Senften et al., 2006) and that CDH23 is a component of kinociliary links (Siemens et al., 2004; Goodyear et al., 2010). Based on these reports, we tested whether Cdh23 was required for GFP-Lhfp15a localization. In *cdh23ⁿ¹⁹* mutants, GFP-Lhfp15 is sparsely distributed throughout the length of the kinocilium ($n = 4/4$ individuals, **Figures 6E,E'**). We also observe a redistribution of GFP-Lhfp15a into the kinocilium using the *cdh23^{tj264}* allele ($n = 4/4$ individuals; **Supplementary Figures 6C,C'**). In both *cdh23* alleles, we see occasional GFP signal in the stereocilia as well, though this localization is not as robust. Interestingly, these results contrast with those from mouse cochlear hair cells which showed that Lhfp15 does not require Cdh23 for bundle localization (Zhao et al., 2014). The same study also could not detect any biochemical interaction between LHFPL5 and proteins of the upper tip link density including CDH23, USH1C/Harmonin, or USH1G/Sans.

Together, our data indicate an unexpected role for Cdh23 in the localization of GFP-Lhfp15a to the region of kinociliary links in zebrafish vestibular hair cells.

Myosin 7A (MYO7A) is an actin-based motor protein required for the localization of many proteins of the hair bundle, including PCDH15 and USH1C/Harmonin, along with several proteins of the Usher type 2 complex (Boëda et al., 2002; Senften et al., 2006; Lefevre et al., 2008; Morgan et al., 2016; Maeda et al., 2017; Zou et al., 2017). Results in both mice and zebrafish suggest that MYO7A is not required for CDH23 bundle localization (Senften et al., 2006; Blanco-Sanchez et al., 2014). However, its role in Lhfp15 localization has not been examined. In *myo7aa^{ty220}* (*mariner*) mutant hair cells, GFP-Lhfp15a localization in hair bundle is severely disrupted ($n = 5/5$ individuals; **Figures 6F,F'**). We observe GFP signal near the base of hair bundles and occasionally in stereocilia (yellow arrowheads), but do not see robust Lhfp15a localization in the presumptive kinociliary links nor to the kinocilium itself. Taken together, our results using the GFP-Lhfp15a transgene suggest that Pcdh15a, Cdh23, and Myo7aa all play distinct roles in Lhfp15 localization in the bundle of zebrafish vestibular hair cells.

DISCUSSION

In this study, we provide support for the following points: (1) The ancestral *lhfp15* gene was likely duplicated as a result of the teleost WGD, leading to the *lhfp15a* and *lhfp15b* ohnologs described in this paper. (2) In zebrafish, there has been subfunctionalization of these genes as a result of their divergent expression patterns. As determined by mRNA *in situ* hybridization, *lhfp15a* is expressed only in auditory and vestibular hair cells of the ear while *lhfp15b* is expressed solely in hair cells of the lateral line organ. Consistent with their expression patterns, we show that each ohnolog mediates mechanotransduction in the corresponding populations of sensory hair cells in zebrafish. (3) Targeting of GFP-tagged Tmcs to the hair bundle is independent of Lhfp15a function. (4) Proper targeting of GFP-tagged Lhfp15a to the hair bundle requires the tip link protein Pcdh15a, but as in mice, Lhfp15a can localize to regions of the hair bundle independently of Pcdh15 function. Additionally, we demonstrate novel requirements for Cdh23 and the Myo7aa motor protein in Lhfp15 localization.

Duplicated Zebrafish Genes in Hair Cell Function

With regards to genes involved in hair cell function, the zebrafish duplicates of *calcium channel, voltage-dependent, L type, alpha 1D* (*cacna1d/cav1.3*), *C-terminal binding protein 2* (*ctbp2/ribeye*), *myosin 6* (*myo6*), *otofelin* (*otof*), *pcdh15*, and *tmc2* have been analyzed genetically. In the cases of *cacna1db*, *pcdh15b* and *myo6a*, these ohnologs are no longer functional in hair cells (Seiler et al., 2004, 2005; Sidi et al., 2004). For the *ctbp2*, *otofelin*, and *tmc2* duplicates, both genes are required in at least partially overlapping populations of hair cells (Sheets et al., 2011; Maeda et al., 2014; Lv et al., 2016; Chou et al., 2017). In contrast, our results for the *lhfp15* ohnologs suggest that each gene is

expressed and functionally required in distinct, non-overlapping hair cell lineages. To our knowledge, this is the first description of duplicated genes whose expression patterns have cleanly partitioned between inner ear and lateral line hair cells.

Subfunctionalization of Zebrafish *lhfp15* Ohnologs

We constructed a phylogenetic tree using publicly available *Lhfp15* protein sequence data (Figure 1). Our results suggest that the ancestral *lhfp15* gene was duplicated during the teleost WGD event and that both genes have been retained throughout the teleost lineage (Figure 1). Our conclusion that *lhfp15a* and *lhfp15b* are ohnologs is substantiated by a recent study of ohnologs in teleosts (Singh and Isambert, 2019). In all four teleost species surveyed, Singh and Isambert show that *lhfp15a* and *lhfp15b* are true ohnologs that arose from the teleost-specific WGD under the strictest criteria used in their study.

Some kind of selection pressure is required for the retention of both gene ohnologs (Glasauer and Neuhauss, 2014). Our *in situ* hybridization results show that *lhfp15a* and *lhfp15b* are expressed in distinct populations of hair cells and support the idea that the zebrafish *lhfp15* ohnologs were retained because of their divergent expression patterns (Figure 2). Analysis of hair cell function in the different *lhfp15* mutants agrees with the gene expression results, showing that *lhfp15a* is required for transduction in the ear while *lhfp15b* plays the same role in the lateral line organs. However, rescue of the MET channel defects in *lhfp15b*^{vo35} mutants by GFP-tagged *Lhfp15a* suggests that the functions of these ohnologs are at least partially interchangeable. This result is not surprising given the high degree of similarity between the *Lhfp15a* and *5b* proteins. As such, the subfunctionalization of the *lhfp15* ohnologs appears to be caused by the divergence in their expression patterns rather than functional differences in their protein products. It is possible that a similar mechanism is responsible for the retention of both genes in other teleost species as well, though the expression patterns of the *lhfp15* ohnologs have not been examined in other fish.

The non-overlapping expression of the *lhfp15* ohnologs provides us with a unique genetic tool to study lateral line function. Most mechanotransduction mutants in zebrafish disrupt both inner ear and lateral line hair cell function (Nicolson, 2017). As such, we are unable to assess the role of the lateral line independently of auditory and vestibular defects, which are lethal for larval fish. The *lhfp15b* mutants are adult viable (data not shown) and represent a possible genetic model for understanding the lateral line in both larval and adult fish. Future studies on adults will determine whether the lateral line remains non-functional and whether *lhfp15b* contributes to inner ear function in the mature auditory and vestibular systems.

The Molecular Requirements for Bundle Localization of MET Complex Proteins Differs Between Mouse and Zebrafish Hair Cells

Our understanding of mechanotransduction at the molecular level is heavily informed by work done using mouse cochlear

hair cells. However, analysis of zebrafish inner ear and lateral line hair cells can lead to a more complete picture of how vertebrate sensory hair cells form the MET complex. At their core, the genetic and molecular bases for mechanotransduction are well conserved between mouse and zebrafish hair cells. For example, the tip link proteins *Cdh23* and *Pcdh15a*, MET channel subunits *Tmc1/2*, *Tmie*, and *Lhfp15*, along with additional factors such as *Tomt*, *Cib2*, and *Myo7aa* are all necessary for MET channel function in both mice and fish (Nicolson et al., 1998; Siemens et al., 2004; Söllner et al., 2004; Senften et al., 2006; Gleason et al., 2009; Kawashima et al., 2011; Xiong et al., 2012; Zhao et al., 2014; Cunningham et al., 2017; Erickson et al., 2017; Giese et al., 2017; Pacentine and Nicolson, 2019). However, while each of these factors are required for mechanotransduction in vertebrate hair cells, the details of how they contribute to MET channel function may differ depending on the particular type of hair cell or the vertebrate species. For example, *Tmie* is required for *Tmc* localization to the hair bundle in zebrafish (Pacentine and Nicolson, 2019), but this does not appear to be the case in mouse cochlear hair cells (Zhao et al., 2014). The evolutionary pressures that lead to these differences between mouse and zebrafish hair cells are not understood.

Based on multiple lines of evidence gathered from mice, *TMC1* and *TMC2* have different requirements for *LHFPL5* regarding localization to the hair bundle (Beurg et al., 2015). Endogenous *TMC1* is absent from the bundle in *LHFPL5*-deficient cochlear hair cells with the remaining MET current mediated through *TMC2*. Exogenously expressed *TMC2* is still targeted correctly in *Lhfp15* mutants, but it was not reported whether the same is true for exogenous *TMC1*, nor whether similar requirements hold for vestibular hair cells. As such, the role of *LHFPL5* in mechanotransduction is not clear: is *LHFPL5* required primarily for targeting *TMC1* to the hair bundle, or does *LHFPL5* mediate MET channel function in other ways?

For our study, we used stable transgenic lines expressing GFP-tagged *Tmc1* and *Tmc2b* to show that the *Tmcs* do not require *Lhfp15a* for targeting to the stereocilia of zebrafish vestibular hair cells. Nor is *Lhfp15b* required for *Tmc2b*-GFP localization in the hair bundle of neuromast hair cells. The occasional FM labeled-hair cell in *lhfp15b* and *lhfp15a/5b* mutant neuromasts is consistent with the continued ability of the *Tmcs* to localize to the hair bundle. This observation is reminiscent of the sporadic, low level of FM dye labeling in the cochlear hair cells of *Lhfp15* mutant mice (György et al., 2017). Partial compensation by yet another member of the *lhfp1* family remains as a possible explanation for the remaining basal channel function. Lastly, we find that exogenous *Tmc* expression does not rescue MET channel activity in either *lhfp15* mutant zebrafish. Taken together, our results support a *Tmc*-independent role for *Lhfp15* proteins in mechanotransduction.

What then is the role of *LHFPL5* in vertebrate mechanotransduction? *LHFPL5* and *PCDH15* are known to form a protein complex and regulate each other's localization to the site of mechanotransduction in mouse cochlear hair cells (Xiong et al., 2012; Mahendrasingam et al., 2017; Ge et al., 2018).

However, their localization to the hair bundle is not completely dependent on one another. For example, tips links are not completely lost in *Lhfp15*^{-/-} cochlear hair cells and exogenous overexpression of PCDH15 partially rescues the transduction defects in *Lhfp15* mutant mice (Xiong et al., 2012). Similarly, a detailed immunogold study in wild type and *Pcdh15*^{-/-} cochlear hair cells showed that there are PCDH15-dependent and PCDH15-independent sites of LHFPL5 localization (Mahendrasingam et al., 2017). PCDH15 is required for stable LHFPL5 localization at the tips of ranked stereocilia in association with the MET channel complex. However, LHFPL5 is still targeted to shaft and ankle links, unranked stereocilia, and the kinocilium in P0-P3 inner and outer hair cells from both wild type and *Pcdh15*^{-/-} mutant mice (Mahendrasingam et al., 2017). Whether the kinocilia localization would remain in mature cochlear hair cells is not known because the kinocilia degenerate by P8 in mice and detailed LHFPL5 localization in vestibular hair cells (which retain their kinocilium) has not been reported.

Zebrafish hair cells retain a kinocilium throughout their life, thus providing a different context in which to examine *Lhfp15* localization. In wild type hair cells, GFP-*Lhfp15a* is present at the tips of the shorter ranked stereocilia, but the most robust signal is detected in the tallest stereocilia adjacent to the kinocilium. In *pcdh15a* mutants, only this “kinocilia link”-like signal remains in the hair bundle. This result is similar to the LHFPL5 localization reported at the tips of the tallest stereocilia of P3 cochlear hair cells from wild type mice, a region where LHFPL5 would presumably not be associated with either PCDH15 or the TMCs (Mahendrasingam et al., 2017). Since the kinocilium does not degenerate in zebrafish hair cells, our results suggest that *Lhfp15a* is normally targeted to these kinocilia links in wild type cells and that its retention at this site does not require *Pcdh15a*. Thus, there are PCDH15-dependent and PCDH15-independent mechanisms of LHFPL5 localization in both mouse and zebrafish hair cells. These results suggest that LHFPL5 performs as-of-yet uncharacterized PCDH15-independent functions as well.

Cdh23 is thought to form part of the linkages between the kinocilium and adjacent stereocilia, and therefore may play a role in retaining *Lhfp15a* at these sites. Consistent with this hypothesis, *cdh23* mutants do not exhibit GFP-*Lhfp15a* accumulation in stereocilia. Instead, GFP-*Lhfp15a* is diffusely distributed throughout the kinocilium. These data suggest that normal *Lhfp15a* localization requires both *Pcdh15a* and *Cdh23* function, albeit in distinct ways. This result differs from previous reports which found that *Lhfp15* still localized to the tips of stereocilia in *CDH23*-deficient cochlear hair cells of mice. The same study also could not detect a biochemical interaction between *Lhfp15* and *CDH23* via co-IP in heterologous cells (Xiong et al., 2012). Given these contrasting results for mouse and zebrafish hair cells, it seems that the requirement for *Cdh23* in the localization of LHFPL5 is not a universal one.

Given the available biochemical evidence, it is possible that the association between *Lhfp15a* and *Cdh23* is indirect

through an as-of-yet unidentified protein or protein complex. Based on the defects in GFP-*Lhfp15a* localization in *myo7aa* mutants, *Myo7aa* is a candidate member of this uncharacterized protein complex. Taken together, these results highlight the fact that, although all sensory hair cells share many core genetic and biochemical features, there are important details that differ between the various types of hair cells and between vertebrate species. Analyzing these differences will allow for a more comprehensive understanding of vertebrate hair cell function and the underlying principles of mechanotransduction.

DATA AVAILABILITY STATEMENT

The datasets generated for this study are available on request to the corresponding author.

ETHICS STATEMENT

The animal study was reviewed and approved by the Institutional Animal Care and Use Committee, Oregon Health & Science University Institutional Animal Care and Use Committee, East Carolina University.

AUTHOR CONTRIBUTIONS

TE and TN conceived and designed the study. TE, IP, AV, and RC collected and analyzed the data. TE wrote the manuscript with Materials and Methods sections contributed by IP and AV and editorial input from TN and IP.

FUNDING

This study was supported by funding from the NIDCD (R01 DC013572 and DC013531 to TN) and from East Carolina University's Division of Research, Economic Development and Engagement (REDE), Thomas Harriot College of Arts and Science (THCAS), and Department of Biology (to TE).

ACKNOWLEDGMENTS

We thank Eliot Smith for assistance with CRISPR-Cas9 knockout of *lhfp15b*. We also thank Leah Snyder, Matthew Esqueda, and members of the Erickson lab for their assistance with animal husbandry.

SUPPLEMENTARY MATERIAL

The Supplementary Material for this article can be found online at: <https://www.frontiersin.org/articles/10.3389/fnmol.2019.00320/full#supplementary-material>

REFERENCES

- Allendorf, F. W., and Thorgaard, G. H. (1984). "Tetraploidy and the evolution of salmonid fishes," in *Evolutionary Genetics of Fishes*, ed. B. J. Turner, (Boston, MA: Springer), 1–53. doi: 10.1007/978-1-4684-4652-4_1
- Beurg, M., Xiong, W., Zhao, B., Müller, U., and Fettiplace, R. (2015). Subunit determination of the conductance of hair-cell mechanotransducer channels. *Proc. Natl. Acad. Sci. U.S.A.* 112, 1589–1594. doi: 10.1073/pnas.1420906112
- Blanco-Sanchez, B., Clement, A., Fierro, J., Washbourne, P., and Westerfield, M. (2014). Complexes of Usher proteins preassemble at the endoplasmic reticulum and are required for trafficking and ER homeostasis. *Dis. Model. Mech.* 7, 547–559. doi: 10.1242/dmm.014068
- Boëda, B., El-Amraoui, A., Bahloul, A., Goodyear, R., Daviet, L., Blanchard, S., et al. (2002). Myosin VIIa, harmonin and cadherin 23, three Usher I gene products that cooperate to shape the sensory hair cell bundle. *EMBO J.* 21, 6689–6699. doi: 10.1093/emboj/cdf689
- Braasch, I., Gehrke, A. R., Smith, J. J., Kawasaki, K., Manousaki, T., Pasquier, J., et al. (2016). The spotted gar genome illuminates vertebrate evolution and facilitates human-teleost comparisons. *Nat. Genet.* 48, 427–437. doi: 10.1038/ng.3526
- Chou, S.-W., Chen, Z., Zhu, S., Davis, R. W., Hu, J., Liu, L., et al. (2017). A molecular basis for water motion detection by the mechanosensory lateral line of Zebrafish. *Nat. Commun.* 8:2234. doi: 10.1038/s41467-017-01604-1602
- Cunningham, C. L., and Müller, U. (2019). Molecular structure of the hair cell mechano-electrical transduction complex. *Cold Spring Harb. Perspect. Med.* 9:a033167. doi: 10.1101/cshperspect.a033167
- Cunningham, C. L., Wu, Z., Jafari, A., Zhao, B., Schrode, K., Harkins-Perry, S., et al. (2017). The murine catecholamine methyltransferase mTOMT is essential for mechanotransduction by cochlear hair cells. *Elife* 6:e33307. doi: 10.7554/eLife.24318
- Dereeper, A., Guignon, V., Blanc, G., Audic, S., Buffet, S., Chevenet, F., et al. (2008). Phylogeny.fr: robust phylogenetic analysis for the non-specialist. *Nucleic Acids Res.* 36, W465–W469. doi: 10.1093/nar/gkn180
- Erickson, T., French, C. R., and Waskiewicz, A. J. (2010). Meis1 specifies positional information in the retina and tectum to organize the Zebrafish visual system. *Neural Dev.* 5:22. doi: 10.1186/1749-8104-5-22
- Erickson, T., Morgan, C. P., Olt, J., Hardy, K., Busch-Nentwich, E., Maeda, R., et al. (2017). Integration of Tmc1/2 into the mechanotransduction complex in Zebrafish hair cells is regulated by Transmembrane O-methyltransferase (Tomt). *Elife* 6:e28474. doi: 10.7554/eLife.28474
- Ernest, S., Rauch, G.-J., Haffter, P., Geisler, R., Petit, C., and Nicolson, T. (2000). Mariner is defective in myosin VIIA: a Zebrafish model for human hereditary deafness. *Hum. Mol. Genet.* 9, 2189–2196. doi: 10.1093/hmg/9.14.2189
- Gagnon, J. A., Valen, E., Thyme, S. B., Huang, P., Ahkmetova, L., Pauli, A., et al. (2014). Efficient mutagenesis by Cas9 protein-mediated oligonucleotide insertion and large-scale assessment of single-guide RNAs. *PLoS One* 9:e98186. doi: 10.1371/journal.pone.0098186
- Ge, J., Elferich, J., Goehring, A., Zhao, H., Schuck, P., and Gouaux, E. (2018). Structure of mouse protocadherin 15 of the stereocilia tip link in complex with LHFPL5. *Elife* 7:e38770. doi: 10.7554/eLife.38770
- Giese, A. P. J., Tang, Y.-Q., Sinha, G. P., Bowl, M. R., Goldring, A. C., Parker, A., et al. (2017). CIB2 interacts with TMC1 and TMC2 and is essential for mechanotransduction in auditory hair cells. *Nat. Commun.* 8:43. doi: 10.1038/s41467-017-00061-61
- Glaser, S. M. K., and Neuhaus, S. C. F. (2014). Whole-genome duplication in teleost fishes and its evolutionary consequences. *Mol. Genet. Genomics* 289, 1045–1060. doi: 10.1007/s00438-014-0889-882
- Gleason, M. R., Nagiel, A., Jamet, S., Vologodskaya, M., López-Schier, H., and Hudspeth, A. J. (2009). The transmembrane inner ear (Tmie) protein is essential for normal hearing and balance in the Zebrafish. *Proc. Natl. Acad. Sci. U.S.A.* 106, 21347–21352. doi: 10.1073/pnas.0911632106
- Goodyear, R. J., Forge, A., Legan, P. K., and Richardson, G. P. (2010). Asymmetric distribution of cadherin 23 and protocadherin 15 in the kinociliary links of avian sensory hair cells. *J. Comp. Neurol.* 518, 4288–4297. doi: 10.1002/cne.22456
- György, B., Sage, C., Indzhukulian, A. A., Scheffer, D. I., Brisson, A. R., Tan, S., et al. (2017). Rescue of hearing by gene delivery to inner-ear hair cells using exosome-associated AAV. *Mol. Ther.* 25, 379–391. doi: 10.1016/j.yymthe.2016.12.010
- Kawashima, Y., Géléoc, G. S. G., Kurima, K., Labay, V., Lelli, A., Asai, Y., et al. (2011). Mechanotransduction in mouse inner ear hair cells requires transmembrane channel-like genes. *J. Clin. Invest.* 121, 4796–4809. doi: 10.1172/JCI60405
- Kazmierczak, P., Sakaguchi, H., Tokita, J., Wilson-Kubalek, E. M., Milligan, R. A., Müller, U., et al. (2007). Cadherin 23 and protocadherin 15 interact to form tip-link filaments in sensory hair cells. *Nature* 449, 87–91. doi: 10.1038/nature06091
- Lefevre, G., Michel, V., Weil, D., Lepelletier, L., Bizard, E., Wolfrum, U., et al. (2008). A core cochlear phenotype in USH1 mouse mutants implicates fibrous links of the hair bundle in its cohesion, orientation and differential growth. *Development* 135, 1427–1437. doi: 10.1242/dev.012922
- Li, X., Yu, X., Chen, X., Liu, Z., Wang, G., Li, C., et al. (2019). Localization of TMC1 and LHFPL5 in auditory hair cells in neonatal and adult mice. *FASEB J.* 33, 6838–6851. doi: 10.1096/fj.201802155RR
- Longo-Guess, C. M., Gagnon, L. H., Cook, S. A., Wu, J., Zheng, Q. Y., and Johnson, K. R. (2005). A missense mutation in the previously undescribed gene Tmhs underlies deafness in hurry-scurry (hscy) mice. *Proc. Natl. Acad. Sci. U.S.A.* 102, 7894–7899. doi: 10.1073/pnas.0500760102
- Lu, Z., and DeSmidt, A. A. (2013). Early development of hearing in Zebrafish. *JARO J. Assoc. Res. Otolaryngol.* 14:509. doi: 10.1007/S10162-013-0386-Z
- Lv, C., Stewart, W. J., Akanyeti, O., Frederick, C., Zhu, J., Santos-Sacchi, J., et al. (2016). Synaptic ribbons require ribeye for electron density, proper synaptic localization, and recruitment of calcium channels. *Cell Rep.* 15, 2784–2795. doi: 10.1016/j.celrep.2016.05.045
- Maeda, R., Kindt, K. S., Mo, W., Morgan, C. P., Erickson, T., Zhao, H., et al. (2014). Tip-link protein protocadherin 15 interacts with transmembrane channel-like proteins TMC1 and TMC2. *Proc. Natl. Acad. Sci. U.S.A.* 111, 12907–12912. doi: 10.1073/pnas.1402152111
- Maeda, R., Pacentine, I. V., Erickson, T., and Nicolson, T. (2017). Functional analysis of the transmembrane and cytoplasmic domains of pcdh15a in Zebrafish hair cells. *J. Neurosci.* 37, 3231–3245. doi: 10.1523/JNEUROSCI.2216-16.2017
- Mahendrasingam, S., Fettiplace, R., Alagramam, K. N., Cross, E., and Furness, D. N. (2017). Spatiotemporal changes in the distribution of LHFPL5 in mice cochlear hair bundles during development and in the absence of PCDH15. *PLoS One* 12:e0185285. doi: 10.1371/journal.pone.0185285
- Morgan, C. P., Krey, J. F., Grati, M., Zhao, B., Fallen, S., Kannan-Sundhari, A., et al. (2016). PDZD7-MYO7A complex identified in enriched stereocilia membranes. *Elife* 5:e18312. doi: 10.7554/eLife.18312
- Nicolson, T. (2017). The genetics of hair-cell function in Zebrafish. *J. Neurogenet* 31, 102–112. doi: 10.1080/01677063.2017.1342246
- Nicolson, T., Rüschi, A., Friedrich, R. W., Granato, M., Ruppertsberg, J. P., and Nüsslein-Volhard, C. (1998). Genetic analysis of vertebrate sensory hair cell mechanosensation: the Zebrafish circler mutants. *Neuron* 20, 271–283. doi: 10.1016/S0896-6273(00)80455-80459
- Obholzer, N., Swinburne, I. A., Schwab, E., Nechiporuk, A. V., Nicolson, T., and Megason, S. G. (2012). Rapid positional cloning of Zebrafish mutations by linkage and homozygosity mapping using whole-genome sequencing. *Development* 139, 4280–4290. doi: 10.1242/dev.083931
- Ohno, S. (1970). *Evolution by Gene Duplication*. Berlin, Heidelberg: Berlin: Springer.
- Pacentine, I. V., and Nicolson, T. (2019). Subunits of the mechano-electrical transduction channel, Tmc1/2b, require Tmie to localize in Zebrafish sensory hair cells. *PLoS Genet.* 15:e1007635. doi: 10.1371/journal.pgen.1007635
- Pan, B., Akyuz, N., Liu, X.-P., Asai, Y., Nist-Lund, C., Kurima, K., et al. (2018). TMC1 forms the pore of mechanosensory transduction channels in vertebrate inner ear hair cells. *Neuron* 99, 736.e6–753.e6. doi: 10.1016/j.neuron.2018.07.033
- Pan, B., Géléoc, G. S., Asai, Y., Horwitz, G. C., Kurima, K., Ishikawa, K., et al. (2013). TMC1 and TMC2 are components of the mechanotransduction channel in hair cells of the mammalian inner ear. *Neuron* 79, 504–515. doi: 10.1016/j.neuron.2013.06.019
- R Core Team (2019). *J. R. A Language and Environment for Statistical Computing*. Vienna: R Core Team.

- RStudio Team (2018). *RStudio: Integrated Development Environment for R*. Vienna: RStudio Team.
- Schneider, C. A., Rasband, W. S., and Eliceiri, K. W. (2012). NIH Image to ImageJ: 25 years of image analysis. *Nat. Methods* 9, 671–675. doi: 10.1038/nmeth.2089
- Seiler, C., Ben-David, O., Sidi, S., Hendrich, O., Rusch, A., Burnside, B., et al. (2004). Myosin VI is required for structural integrity of the apical surface of sensory hair cells in Zebrafish. *Dev. Biol.* 272, 328–338. doi: 10.1016/j.ydbio.2004.05.004
- Seiler, C., Finger-Baier, K. C., Rinner, O., Makhankov, Y. V., Schwarz, H., Neuhaus, S. C. F., et al. (2005). Duplicated genes with split functions: independent roles of protocadherin15 orthologues in Zebrafish hearing and vision. *Development* 132, 615–623. doi: 10.1242/dev.01591
- Senften, M., Schwander, M., and Kazmierczak, P. (2006). Physical and functional interaction between protocadherin 15 and myosin VIIa in mechanosensory hair cells. *J. Neurosci.* 26, 2060–2071. doi: 10.1523/JNEUROSCI.4251-05.2006
- Shabbir, M. I., Ahmed, Z. M., Khan, S. Y., Riazuddin, S., Waryah, A. M., Khan, S. N., et al. (2006). Mutations of human TMHS cause recessively inherited non-syndromic hearing loss. *J. Med. Genet.* 43, 634–640. doi: 10.1136/jmg.2005.039834
- Sheets, L., Trapani, J. G., Mo, W., Obholzer, N., and Nicolson, T. (2011). Ribeye is required for presynaptic CaV1.3a channel localization and afferent innervation of sensory hair cells. *Development* 138, 1309–1319. doi: 10.1242/dev.059451
- Sidi, S., Busch-Nentwich, E., Friedrich, R., Schoenberger, U., and Nicolson, T. (2004). gemini encodes a Zebrafish L-type calcium channel that localizes at sensory hair cell ribbon synapses. *J. Neurosci.* 24, 4213–4223. doi: 10.1523/JNEUROSCI.0223-04.2004
- Siemens, J., Lillo, C., Dumont, R. A., Reynolds, A., Williams, D. S., Gillespie, P. G., et al. (2004). Cadherin 23 is a component of the tip link in hair-cell stereocilia. *Nature* 428, 950–955. doi: 10.1038/nature02483
- Singh, P. P., and Isambert, H. (2019). OHNOLOGS v2: a comprehensive resource for the genes retained from whole genome duplication in vertebrates. *Nucleic Acids Res.* gkz909 doi: 10.1093/nar/gkz909
- Söllner, C., Rauch, G.-J., Siemens, J., Geisler, R., Schuster, S. C., Müller, U., et al. (2004). Mutations in cadherin 23 affect tip links in Zebrafish sensory hair cells. *Nature* 428, 955–959. doi: 10.1038/nature02484
- Thisse, C., and Thisse, B. (2008). High-resolution in situ hybridization to whole-mount Zebrafish embryos. *Nat. Protoc.* 3, 59–69. doi: 10.1038/nprot.2007.514
- Westerfield, M. (2000). *The Zebrafish Book. A Guide for the Laboratory Use of Zebrafish (Danio Rerio)*, 4th Edn. Eugene OR: University of Oregon.
- Wickham, H. (2016). *Ggplot2: Elegant Graphics for Data Analysis*. New York, NY: Springer-Verlag.
- Wolfe, K. (2000). Robustness—it's not where you think it is. *Nat. Genet.* 25, 3–4. doi: 10.1038/75560
- Xiong, W., Grillet, N., Elledge, H. M., Wagner, T. F. J., Zhao, B., Johnson, K. R., et al. (2012). TMHS is an integral component of the mechanotransduction machinery of cochlear hair cells. *Cell* 151, 1283–1295. doi: 10.1016/j.cell.2012.10.041
- Yao, Q., DeSmidt, A. A., Tekin, M., Liu, X., and Lu, Z. (2016). Hearing assessment in Zebrafish during the first week postfertilization. *Zebrafish* 13, 79–86. doi: 10.1089/ZEB.2015.1166
- Zhao, B., Wu, Z., Grillet, N., Yan, L., Xiong, W., Harkins-Perry, S., et al. (2014). TMIE is an essential component of the mechanotransduction machinery of cochlear hair cells. *Neuron* 84, 954–967. doi: 10.1016/j.neuron.2014.10.041
- Zou, J., Chen, Q., Almishaal, A., Mathur, P. D., Zheng, T., Tian, C., et al. (2017). The roles of USH1 proteins and PDZ domain-containing USH proteins in USH2 complex integrity in cochlear hair cells. *Hum. Mol. Genet.* 26, 624–636. doi: 10.1093/hmg/ddw421

Conflict of Interest: The authors declare that the research was conducted in the absence of any commercial or financial relationships that could be construed as a potential conflict of interest.

Copyright © 2020 Erickson, Pacentine, Venuto, Clemens and Nicolson. This is an open-access article distributed under the terms of the Creative Commons Attribution License (CC BY). The use, distribution or reproduction in other forums is permitted, provided the original author(s) and the copyright owner(s) are credited and that the original publication in this journal is cited, in accordance with accepted academic practice. No use, distribution or reproduction is permitted which does not comply with these terms.